Korean J. Chem. Eng., **31**(12), 2124-2129 (2014)
DOI: 10.1007/s11814-014-0322-x
pISSN: 0256-1115
eISSN: 1975-7220

RAPID COMMUNICATION

Characterizations of furfuryl alcohol oligomer/polymerization catalyzed by homogeneous and heterogeneous acid catalysts

Taejin Kim*,,***†, Jiwon Jeong***, Mohammed Rahman*, Elaine Zhu*, and Devinder Mahajan*,****

*Chemical and Molecular Engineering Department, Stony Brook University, Stony Brook, NY 11794, USA
**Materials Science and Engineering Department, Stony Brook University, Stony Brook, NY 11794, USA
***Chemistry Department, Stony Brook University, Stony Brook, NY 11794, USA
(*Received 13 August 2014 • accepted 29 October 2014*)

Abstract–The liquid-phase oligomer/polymerization of furfuryl alcohol (FA) catalyzed by homogeneous and heterogeneous acid catalysts was investigated by Infrared (IR) spectroscopy. At room temperature and 100 °C, FA was not decomposed with metal oxide catalysts except for tungsten oxide, whereas amberlyst and sulfuric acid converted a furfuryl alcohol monomer into oligomer/polymer even at a room temperature. During FA oligomer/polymerization reaction, a strong C=O band observed in the IR spectra provided a diketone structure, which was not observed in the Raman spectroscopy. Based on the FA monomer color changings and IR spectra, tungsten oxide can be possibly applied as a heterogeneous catalyst for controlling the product distribution and avoiding a product separation issue from catalyst.

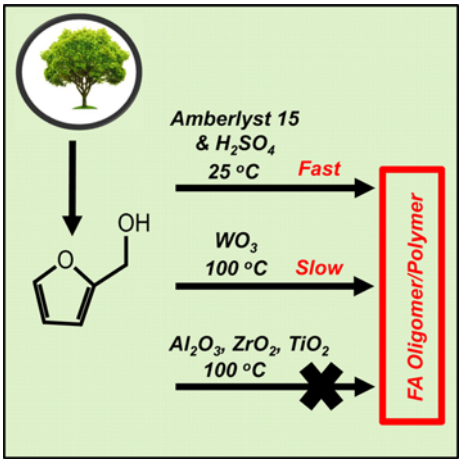

Keywords: Furfuryl Alcohol, Oligomer/Polymerization, Metal Oxide, Heterogeneous, Homogeneous, Infrared Spectroscopy

INTRODUCTION

Biomass is a renewable and sustainable resource that can be converted into bio-chemicals and bio-fuels [1]. The dehydration, rehydration and hydrogenation of the cellulose and hemicellulose lead to a key platform chemicals such as hydroxymethylfurfural (HMF, $C_6H_6O_3$) and furfuryl alcohol (FA, $C_5H_6O_2$), respectively [2,3]. HMF and FA can also converted into levulinic acid (LA, $C_5H_8O_3$), which is one of the top 12 promising biomass derived platform chemicals [4,5] and formic acid [6]. In addition to LA, during acid-catalyzed and hydrothermal reaction, HMF and FA can be also converted into an undesired side product, carbonaceous oligomer and polymer, known as humin, which reduces the selectivity of LA [7,8]. However, from the material point of view, humin is an attractive precursor for carbon nanotube, membrane, carbon fibers, and ordered mesoporous carbons production [9-16]. It has been proposed that 2,5-dioxo-6-hydroxyhexanal (DHH) and carbocation are intermediate monomers during the HMF and FA, respectively, conversion reaction into humin [3,17,18]. The steps involved in the process are shown in Scheme 1.

The chemical structures and morphology of the PFA and PFA derived carbon were demonstrated by multiple characterization investigation: Raman spectroscopy [3,19-21], FT-IR spectroscopy [22,23], UV-visible spectroscopy [24], solid-state ^{1}H and ^{13}C-NMR spectroscopy [22,23], high-performance liquid chromatography [24], scanning electron microscope (SEM) [11], and high-resolution transmission electron microscopy (HRTEM) [25]. According to the reported polymerized structures, the humin structure contains methylene linkage furan rings [26,27], dimethylene ether linkage [20], γ-diketone [28], conjugated double bond sequence [3,23,29], and branched species [30,31]. Even though proposed structures were contradictory in some respects, the observed sample's color, which is dark gray or black, and viscous character were commonly agreed. Many investigations have been made to understand polymeriza-

†To whom correspondence should be addressed.
E-mail: taejin.kim@stonybrook.edu

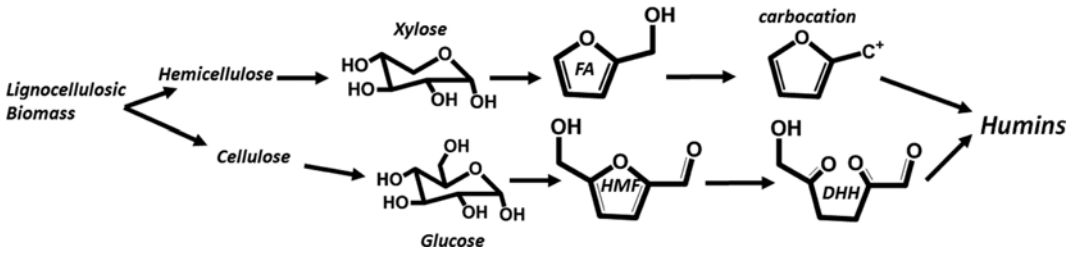

Scheme 1. Reaction pathways for conversion of biomass to humins.

tion mechanisms, to find an intermediate species, and to develop new carbon materials using a sulfuric acid, hydrochloric acid, and phosphoric acid catalysts [3,7,8,14,32,33], which are environmentally unfavorable due to the catalyst separation difficulty from products and toxicity. Although previous studies investigated the homogeneous catalytic activity, to our knowledge, heterogeneous catalysts have not been investigated much. We report here a preliminary study of FA polymerization reaction using metal oxide and present the feasibility of using metal oxide catalysts with spectroscopic techniques.

EXPERIMENTAL

Furfuryl alcohol (FA, 98%), titanium (IV) oxide (≥99%), aluminum oxide (≥98%), zirconium (IV) oxide (99%), Amberlyst 15 ion-exchange resin, and sulfuric acid (99.999%) were obtained from Sigma-Aldrich and used without further purification. In a typical FA polymerization reaction experiment, 3.00 g FA was placed in six clean vials and mixed with 0.3 g of metal oxide catalysts, 0.3 g of Amberlyst 15, and 0.03 g of sulfuric acid catalyst. The six vials, which included a magnetic stir bar, were stirred on Mag-mix stirrer during the reaction. Two batches of six samples were prepared to collect the FTIR spectra and to observe the samples color changing. Infrared spectra were acquired using a Perkin Elmer Frontier FTIR spectrophotometer equipped with an attenuated total reflectance (ATR) accessory. IR spectrum was obtained by averaging 5 scans taken with 0.4 cm^{-1} resolution for both the background, air, and the samples.

RESULTS AND DISCUSSION

1. Color Change of FA Monomer with Acidic Catalysts

The effect of acid metal oxides, Amberlyst, and conc. H_2SO_4 on FA oligomer/polymerization was investigated by FA monomer samples color changes at room temperature and 100 °C. Table 1 shows the notation and the amounts of catalyst and FA used in the experiments. Fig. 1(a) shows the color change of FA samples at room temperature and 100 °C left to oligomer/polymerize over a period of 2 and 1 hr, respectively. At room temperature, the original FA color was not changed over metal oxide catalysts (FTi, FWo, FAl and FZr), while FAmb and FS samples' color was changed to black. These results provided that FAmb and FS samples contained con-

Table 1. Samples notation at different acidic catalysts (metal oxides, Amberlyst, and sulfuric acid). All reactions were at room temperature and 100 °C at ambient pressure

Sample notation	Reactant	Catalysts	Weight (g)
FTi	Furfuryl alcohol	TiO_2	0.30
FWo	3.00 g	WO_3	0.30
FAl		Al_2O_3	0.30
FZr		ZrO_2	0.30
FAmb		Amberlyst 15	0.30
FS		Conc H_2SO_4	0.03

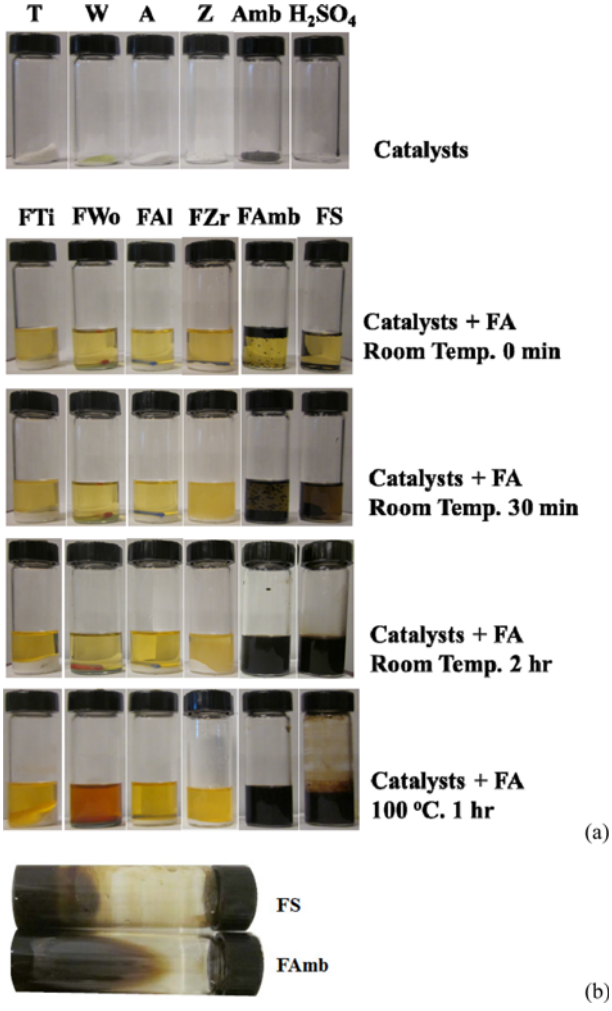

Fig. 1. FA samples (FTi, FWo, FAl, FZr, FAmb, and FS) (a) color changes at room temperature and 100 °C. Furfuryl alcohol (3.00 g), metal oxide catalysts (0.30 g), Amberlyst 15 (0.30 g) and conc. sulfuric acid (0.03 g) (b) viscosity comparison (visual observation) of FS and FAmb at 100 °C 1 hr.

jugated double bond or diketone molecular structures because unconjugated structure should be colorless [3,19,22,28]. Even at 100 °C, most metal oxide catalysts did not make the original FA color change except for FWo. The color of FWo sample continuously changed to reddish color during the reaction. At 100 °C, FAmb and FS samples viscosity increased with time, while FS sample's viscosity is higher than FAmb one (See Fig. 1(b)). This visual observation result provides the following catalytic reactivity for FA oligomer/polymerization reaction: FS>FAmb>>FWo>FTi, FAl, FZr.

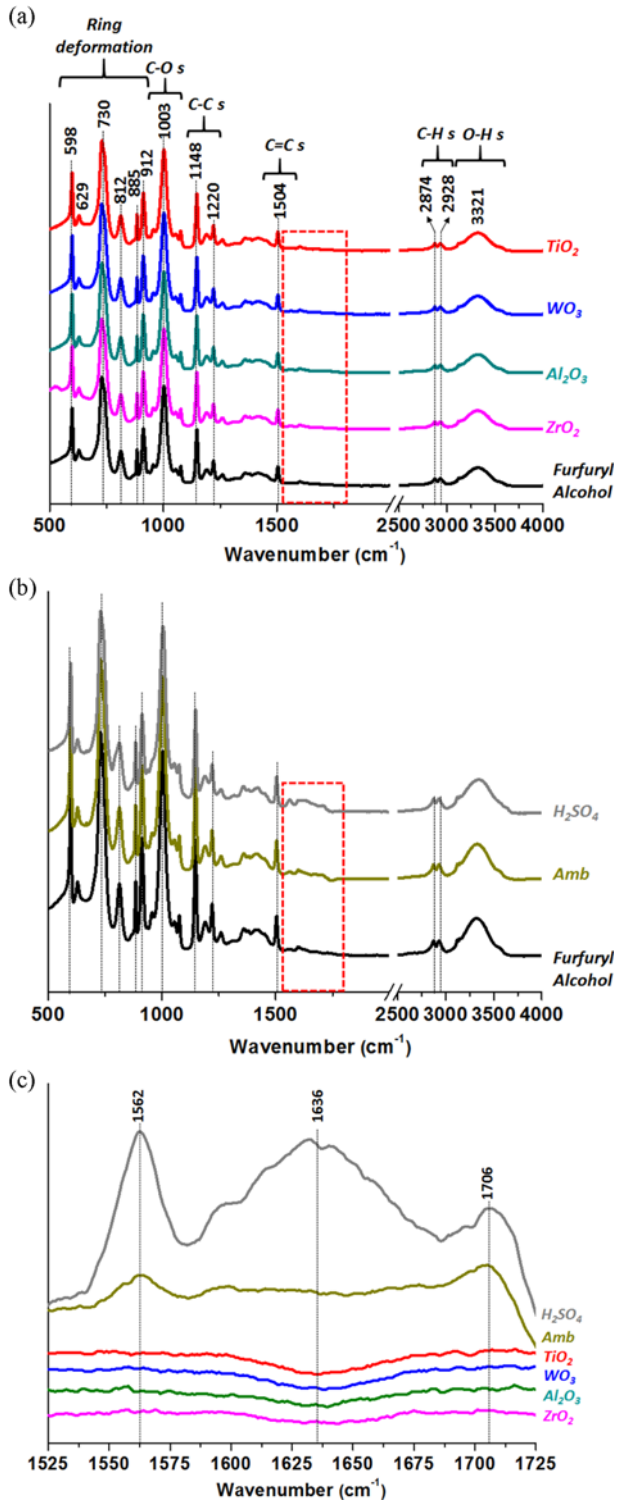

Fig. 2. FTIR spectra of the (a) furfuryl alcohol (3.00 g) and metal oxide catalysts (0.30 g) in the 500-4,000 cm^{-1} region, (b) furfuryl alcohol (3.00 g), amberlyst 15 (0.30 g) and conc. sulfuric acid (0.03 g) solution in the 500-4,000 cm^{-1} region, (c) difference of IR spectra between furfuryl alcohol and catalysts in the 1500-1,800 cm^{-1} region. Reaction conditions: Temp =room temperature, Pressure=atmosphere, Time=2 hr.

2. Chemical Structure Characterization

Oligomer/polymerization of the FA monomer over metal oxide, acidic resin, and mineral acid was investigated by IR to understand the FA structure evolution. The ATR-IR spectra from a series of mixed FA with metal oxides catalyst at room temperature are presented along with the spectrum of FA in Fig. 2(a). TiO_2, WO_3, Al_2O_3, and ZrO_2 metal oxides were used because these catalysts are considered as an acid catalysts [34-41]. In all ranges, no significant peak intensity and shift changes were observed. These results provide that FA will not decompose with metal oxides under the present experimental conditions: room temperature, atmosphere pressure, and 2 hr reaction time. We can expect that temperature or acidity was not high enough to overcome an activation energy for FA conversion into oligomer/polymer, while sulfuric acid can convert FA into low molecular oligomer at room temperature [42]. Wewerka et al., reported difuryl methane, difurfuryl ether, 4-furfuryl-2-pentenoic acid, and 2,5-difurfuryl furan formation from FA over a γ-alumina catalyst at 170 °C [43]. Based on this article, we can hypothesize that reaction temperature is the critical parameter of FA oligomer/polymerization reaction over the metal oxide catalysts.

The IR spectrum contains several high intensity peaks at ~598, ~730, 1,003, and 1,148 cm^{-1}, which are assigned to the furan ring out-of-plane bend, furan ring-CH out-of-plane bend, C-O stretching, and C-C stretching modes, respectively [33,47]. The medium-sized bands between 800 and 920 cm^{-1} are attributed to furan ring-CH out-of-plane bend, furan-CCC in-plane bend [16,32,44]. The bands at ~1,504, ~3,000, and ~3,321 cm^{-1} are attributed to furan-C=C stretching, C-H stretching, O-H stretching band, respectively [3,42,45]. Compared to the other bands, C=C and C-H bands intensities are very weak, which show the highest and medium-sized intensities in the Raman spectra [45]. It can be explained that the energy change between vibrational levels may be Raman active but IR inactive, though both methods provide molecular structure information. In addition to peak intensity difference, FA Raman spectrum does not show hydroxyl vibration (O-H stretching), which is found in the IR spectrum at ~3,321 cm^{-1} [19,20,45].

Fig. 2(b) shows the IR spectra of the oligomer/polymerized FA over Amberlyst 15 and conc. H_2SO_4 catalysts. Experimental conditions were the same as the metal oxides ones. Similar to the Fig. 2(a) results, Amberlyst 15 and conc. H_2SO_4 catalyzed FA IR spectra also contained most FA monomer's IR bands. Peak intensity ratios of the different functional groups and wavenumbers were also very similar to the FA monomer ones. However, new bands were shown in between 1,500 and 1,800 cm^{-1}. To distinguish the new peaks, a subtraction was applied between FA monomer IR spectrum and catalyzed sample's spectrum.

Fig. 2(c) clearly shows the new bands at 1,562, 1,630 and 1,705 cm^{-1} in the 1,500-1,800 cm^{-1} region. The assignment of 1562 cm^{-1} is contradictory in some respects. Yao et al. observed absorption band at 1,559 cm^{-1} and assigned it to the C=C stretching mode in the 2-

5 disubstituted furanic rings [32]. By using IR and Raman spectrometers, Bertarione et al. reported three different wavenumbers at 1,565 cm^{-1} (HCl at 80 °C, IR), 1,560 cm^{-1} (HCl at 25 °C, Raman) and 1,575 cm^{-1} (H-Y zeolite at 25 °C, IR), which are relevant to 1,562 cm^{-1}. Even though wavenumbers were different, authors concluded that these peaks could be ascribed to C=C stretching vibration of the coexistence carbocationic oligomeric and neutral species [19,20]. Recently, Kim et al. compared measured Raman spectra during the FA oligomer/polymerization reaction to the theoretically calculated Raman spectra [3]. On the basis of calculated Raman spectra with conjugated diene structure, they suggested that 1,556 and 1,567 cm^{-1} bands are attributed to the C=C stretching vibration mode inside furan ring structure. From these references, we can conclude that the observed ~1,562 cm^{-1} peak should be assigned C=C stretching mode, while molecular structure is not clear.

In addition to ~1,562 cm^{-1} band assignment, the band assignment of ~1,636 cm^{-1} was controversial and it was assigned to the H_2O bending mode [46], C=O stretching vibrations of bifuryl ketonic species [28], or C=C stretch in the FA polymer [3,19,47]. Because it was reported that ~1,636 cm^{-1} band was observed at higher reaction temperature, first we can avoid the possibility of the H_2O bending mode. Even though the C=O stretch band can be found broad ranges (1,650-1,800 cm^{-1}), we can also avoid the possibility of C=O stretch mode for ~1,636 cm^{-1}, because the C=O stretch mode is generally shown between 1,700 and 1,750 cm^{-1} in ketone group. Based on these two reasons, we can hypothesize that ~1,636 cm^{-1} band is related to the C=C stretching mode.

The weak band at ~1,706 cm^{-1} can be assigned to the C=O stretching vibration, which was not observed by the Raman spectroscopy [3,12,19-21,28,29]. It has been proposed that the C=O bond can be formed due to the furan ring opening by the acid catalyzed reaction [29]. Conley et al. also hypothesized that FA polymer included the combined γ-diketone and methylene bridged polycondensate structure and assigned the band at ~1,710 cm^{-1} is C=O stretching vibration from ketone structure [28]. In addition to γ-diketone and methylene structure, several molecular structures of FA polymer, such as conjugated diene, ether-bridged, and internal OH, were also proposed and confirmed by theory calculation and experimental results [3,22,26,42]. It was also proposed that FA polymer contains a branched or cross-linked polymer as well as a linear structure [15].

3. Temperature Effect on FA Oligomer/Polymer Chemical Structure

It has been proposed that the initial protonation is thermodynamically unfavorable, ΔG=19.2 kJ/mol, and higher temperature is required for FA decomposition into carbonaceous materials [3]. At higher temperature (>400 °C), Raman spectroscopy study of the FA polymerization with a mineral acid reported two broad bands at ~1,600 and ~1,300 cm^{-1}, assigned to the D and G bands, respectively [9,21,48]. Because the molecular structure of FA was changed very quickly at such a high temperature, we chose a mild reaction temperature, 100 °C, and compared the IR spectra to room temperature ones. Fig. 3(a) shows the IR spectra of FA heat treated at 100 °C for 1 hr over metal oxides, Amberlyst, and conc. H_2SO_4 catalysts from 500 to 4,000 cm^{-1}. To compare the catalyzed FA samples IR spectra, all of the spectra were normalized by using the ~1,504 cm^{-1} band of the FA as an internal standard. FA IR spectra were not changed over the metal oxide catalysts at 100 °C. This result explained that

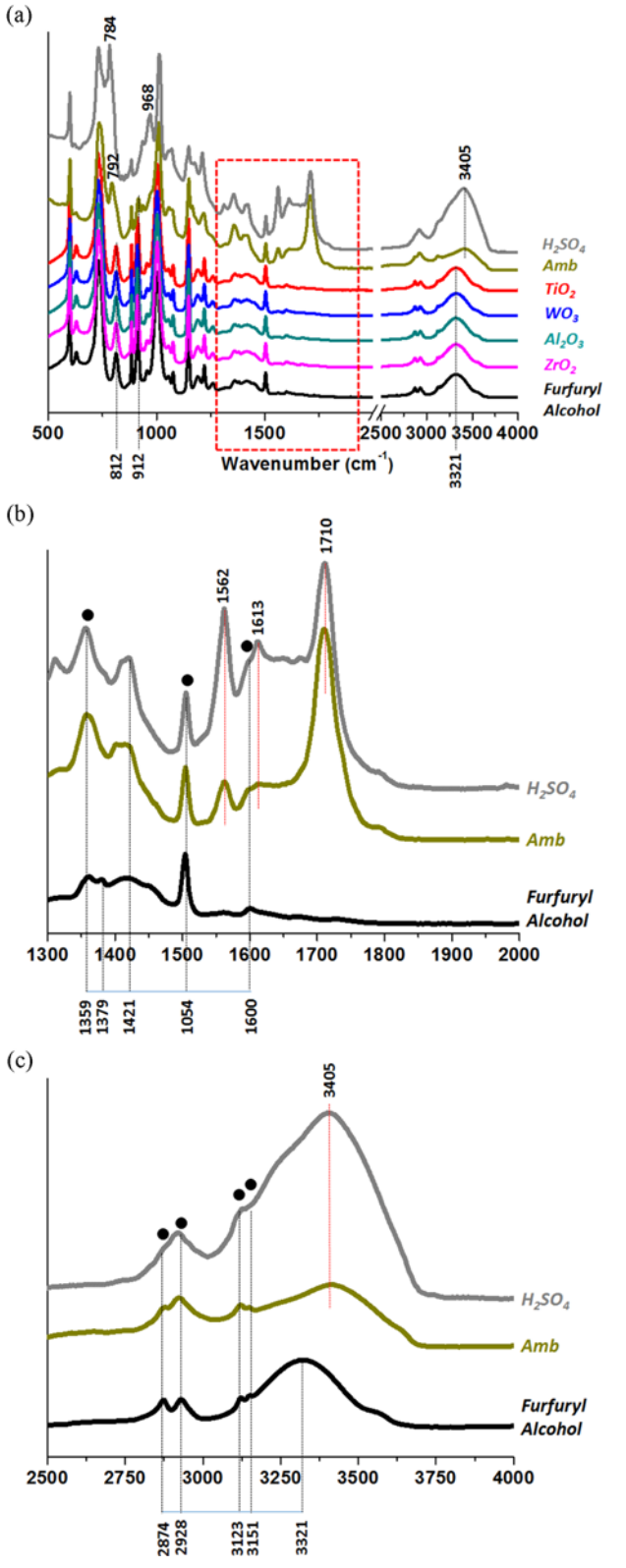

Fig. 3. Infrared spectra of the FA at room temperature and FA oligomer/polymer at 100 °C (a) 500-4,000 cm^{-1} region (b) 1,300-2,000 cm^{-1} region (c) 2,500-4,000 cm^{-1} region. Reaction time; 1 hr.

100 °C was still not enough for the FA decomposition. Although WO_3 catalyzed FA sample color was changed to orange from yel-

low, we can hypothesize that the conversion of FA monomer was very low (see Fig. 1). Compared to metal oxide catalysts, Amberlyst and H_2SO_4 catalyzed FA IR spectra showed several new peaks at different wavenumbers. Due to the complicated peak assignment, in the present work, we mainly report 1) the wavenumber of new peak and 2) peak shift. At 100 °C, FA monomer sample's ~812 cm^{-1} peak, which was assigned to C-H wagging and twisting (w/t) modes in ring structure, disappeared and new peaks appeared at 792 and 784 cm^{-1} over Amberlyst and conc. H_2SO_4, respectively. We can also assumed that ~812 cm^{-1} peak shifted to lower wavenumbers during the oligomer/polymerization reaction. Although we could not assign these peaks clearly, because furan derivatives' (furan and FA) C-H w/t mode were observed at 750-850 cm^{-1}, both 792 and 784 cm^{-1} can be also assigned to C-H w/t mode in ring structure. Fig. 3(a) clearly shows higher C-H w/t peak intensity in conc. H_2SO_4 catalyzed FA IR spectrum. The peak intensity ratio ($I_{C\text{-}H\ w/t}/I_{1504}$) increases in the following order: FA, FA+metal oxides (I_{812}/I_{1504}; ~1.6) <FA+Amberlyst (I_{792}/I_{1504}; ~2.6)<FA+conc. H_2SO_4 (I_{784}/I_{1504}; ~6.5). Compared to the other spectra, the H_2SO_4-catalyzed FA spectrum also contains a unique peak at ~968 cm^{-1} which was not assigned. The most critical wavenumber ranges are 1,300-2,000 cm^{-1}, which provide the possible oligomer/polymer's molecular structure information. In this region, Amberlyst and conc. H_2SO_4 catalyzed FA spectra show strong bands at 1,562 and 1,710 cm (see Fig. 3(b)). Note that in the previous section, these two peaks are not clearly observed at room temperature and distinguished only after subtraction procedure with FA. However, Fig. 3(b) shows and supports that FA oligomer/polymer species contains C=C (closed ring) and C=O (open ring) stretching modes. Similar to ~1,630 cm^{-1} peak, we assume that ~1,613 cm^{-1} peak relates to a C=C stretching mode in furan ring structure. In the 2,500-4,000 cm^{-1} region, four C-H stretching bands in FA spectrum were combined and shown broad peaks in conc. H_2SO_4 spectrum (see Fig. 3(c)). After heat treatments at 100 °C with conc. H_2SO_4 and Amberlyst catalysts, typical O-H stretching band, ~3,321 cm^{-1}, in FA spectrum was shifted to higher wavenumber, ~3,405 cm^{-1}. It has been observed that the adjacent functional group or bond length affects the O-H stretching wavenumber. For instance, lignin, polymer of aromatic alcohols, O-H stretching band was observed between 3,400-3,450 cm^{-1}, which is higher than simple aromatic and aliphatic alcohol's O-H band position, such as phenol (~3,229 cm^{-1}), cyclohexanol (~3,331 cm^{-1}) and butanol (~3,333 cm^{-1}) [49]. Although wavenumber was not reported, Zardin et al. observed free-PFA O-H stretching band at ~3,400 cm^{-1} [21]. Therefore, the shift of the O-H band is related to the oligomer/polymerization of the FA monomer to PFA. To get more information of the oligomer/polymerized products, a detailed gas chromatography and mass spectrometry study is in progress.

CONCLUSIONS

We investigated the furfuryl alcohol (FA) oligomer/polymerization reaction with metal oxides, sulfuric acid, and Amberlyst by means of infrared spectroscopy. At lower reaction temperatures, room temperature and 100 °C, FA oligomer/polymerization reaction was not observed with acidic metal oxide catalysts, while sulfuric acid and Amberlyst catalysts converted FA monomer into FA oligomer/polymer. A strong IR peak at ~1,710 cm^{-1} suggested the evidence of C=O bond in an open ring structure (diketone), which was not observed by Raman spectroscopy. This observation confirmed that to understand the FA oligomer/polymerization reaction mechanism, both Raman and IR spectroscopy techniques should be provided. Sample colors of FA and viscosity were also supported the formation of FA oligomer/polymer: yellow→brown→black. Although no oligomer/polymerization was observed with metal oxide catalysts in the IR spectra, FA sample color change with tungsten oxide catalyst suggested that small amount of FA converted into oligomer/polymer.

ACKNOWLEDGEMENTS

We gratefully acknowledge the financial support for this study from the Department of Materials Science & Engineering and the Program in Chemical and Molecular Engineering at Stony Brook University through startup research funding.

REFERENCES

1. G. W. Huber, J. N. Chheda, C. J. Barrett and J. A. Dumesic, *Science*, **308**, 1446 (2005).
2. N. Shi, Q. Liu, Q. Zhang, T. Wang and L. Ma, *Green Chem.*, **15**, 1967 (2013).
3. T. Kim, R. S. Assary, C. L. Marshall, D. J. Gosztola, L. A. Curtiss and P. C. Stair, *ChemCatChem*., **3**, 1451 (2011).
4. T. Werpy and G. Petersen, Top Value Added Chemicals from Biomass, US Department of Energy, Office of Scientific and Technical Information, Oak Ridge, TN, 2004, No. DOE/GO-102004-1992, http://www.nrel.gov/docs/fy04osti/35523.pdf.
5. J. J. Bozell and G. R. Peterson, *Green Chem.*, **12**, 539 (2010).
6. G. M. G. Maldonado, R. S. Assary, J. Dumesic and L. A. Curtiss, *Energy Environ. Sci.*, **5**, 6981 (2012).
7. S. K. R. Patil and C. R. F. Lund, *Energy Fuels*, **25**, 4745 (2011).
8. S. K. R. Patil, J. Heltzel and C. R. F. Lund, *Energy Fuels*, **26**, 5281 (2012).
9. L. Radhakrishnan, J. Reboul, S. Furukawa, P. Srinivasu, S. Kitagawa and Y. Yamauchi, *Chem. Mater.*, **23**, 1225 (2011).
10. I. S. Park, M. Choi, T. W. Kim and R. Ryoo, *J. Mater. Chem.*, **16**, 3409 (2006).
11. B. Yi, R. Rajagopalan, H. C. Foley, U. J. Kim, X. Liu and P. C. Eklund, *J. Am. Chem. Soc.*, **128**, 11307 (2006).
12. X. H. Men, Z. Z. Zhang, H. J. Song, K. Wang and W. Jiang, *Comp. Sci. Technol.*, **68**, 1042 (2008).
13. J. Yao, H. Wang, J. Liu, K. Y. Chan, L. Zhang and N. Xu, *Carbon*, **43**, 1709 (2005).
14. Y. R. Dong, N. Nishiyama, Y. Egashira and K. Ueyama, *Ind. Eng. Chem. Res.*, **46**, 4040 (2007).
15. H. T. Wang and J. F. Yao, *Ind. Eng. Chem. Res.*, **45**, 6393 (2006).
16. L. He, D. Li, G. Zhang, A. A. Webley, D. Zhao and H. Wang, *Ind. Eng. Chem. Res.*, **49**, 4715 (2010).
17. J. Horvat, B. Klaic, B. Metelko and V. Sunjic, *Tetrahedron Lett.*, **26**, 2111 (1985).
18. J. Horvat, B. Klaic, B. Metelko and V. Sunjic, *Croat. Chem. Acta*, **59**, 429 (1986).
19. S. Bertarione, F. Bonino, F. Cesano, A. Damin, D. Scarano and A. Zecchina, *J. Phys. Chem. B*, **112**, 2580 (2008).

20. S. Bertarione, F. Bonino, F. Cesano, S. Jain, M. Zanetti, D. Scarano and A. Zecchina, *J. Phys. Chem. B*, **113**, 10571 (2009).
21. A. J. G. Zarbin, R. Bertholdo and M. A. F. C. Oliveira, *Carbon*, **40**, 2413 (2002).
22. M. Choura, N. M. Belgacem and A. Gandini, *Macromolecules*, **29**, 3839 (1996).
23. R. Gonzalez, J. M. Figueroa and H. Gonzalez, *European Poly. Journal*, **38**, 287 (2002).
24. Y. R. Swasti and M. Murkovic, *Food Funct*., **3**, 965 (2012).
25. M. S. Kane, J. F. Goellner and H. C. Foley, *Chem. Mater.*, **8**, 2159 (1996).
26. A. P. Dunlop and F. N. Peters, The Furans; Reinhold Publishing Co., New York (1953).
27. C. Moreau, M. N. Belgacem and A. Gandini, *Top. Catal.*, **27**, 11 (2004).
28. R. T. Conley and I. Metil, *J. Appl. Polym. Sci.*, **7**, 37 (1963).
29. I. S. Chung, G. E. Maciel and G. E. Myers, *Macromolecules*, **17**, 1087 (1984).
30. M. Principe, P. Ortis and R. Martinez, *Polym. Int.*, **48**, 637 (1999).
31. T. De la C. Garcia, M. R. Gomez, R. Martinez and C. Alonso, *Polym. Int.*, **52**, 86 (2003).
32. J. Yao, H. Wang, J. Liu, K. Y. Chan, L. Zhang and N. Xu, *Carbon*, **43**, 1709 (2005).
33. E. M. Wewerka, *J. Appl. Polym. Sci.*, **12**, 1671 (1968).
34. C. L. Thomas, Catalytic Processes and Proven Catalysts, Academic Press, New York (1970).
35. C. N. Satterfield, *Heterogeneous Catalysis in Practice*, McGraw-Hill, New York (1980).
36. K. Tanabe, M. Misono, H. Hattori and Y. Ono, New Solid Acids and Bases, Elsevier, **51** (1989).
37. M. Hino and K. Arata, *J. Chem. Soc. Chem. Commun*., **18**, 1259 (1988).
38. J. G. Santiesteban, J. C. Vartuli, S. Han, R. D. Bastian and C. D. Chang, *J. Catal*., **168**, 431 (1997).
39. M. Hino and K. Arata, *Chem. Lett.*, **6**, 971 (1989).
40. T. Kim, A. Burrows, C. Kiely and I. E. Wachs, *J. Catal.*, **246**, 370 (2007).
41. I. E. Wachs, T. Kim and E. I. Ross, *Catal. Today*, **116**, 162 (2006).
42. T. Kim, R. S. Assary, R. E. Pauls, C. L. Marshall, L. A. Curtiss and P. C. Stair, *Catal. Commun.*, **46**, 66 (2014).
43. E. M. Wewerka, E. D. Loughran and K. L. Walters, *J. Appl. Polym. Sci.*, **15**, 1437 (1971).
44. S. Barsberg and R. W. Berg, *J. Phys. Chem. A*, **110**, 9500 (2006).
45. T. Kim, R. S. Assary, L. A. Curtiss, C. L. Marshall and P. C. Stair, *J. Raman Spectrosc.*, **42**, 2069 (2011).
46. A. Zecchina, F. Geobaldo, G. Spoto, S. Bordiga, G. Ricchiardi, R. Buzzoni and G. Petrini, *J. Phys. Chem.*, **100**, 16584 (1996).
47. Z. Wang, Z. Lu, X. Huang, R. Xue and L. Chen, *Carbon*, **36**, 51 (1998).
48. Z. Wang, Z. Lu, Y. Huang, R. Xue, X. Huang and L. Chen, *J. Appl. Phys.*, **82**, 5705 (1997).
49. W. Hoareau, W. G. Trindade, B. Siegmund, A. Castellan and E. Frollini, *Polym. Degrad. Stab.*, **86**, 567 (2004).